ELEPHANT MORAINE 14017: A NEW PRIMITIVE ORDINARY CHONDRITE FROM ANTARCTICA.

C. Park[1], S. Y. Park[1,2], H. Kim[1], and J. I. Lee[1], [1]Division of Earth Sciences, Korea Polar Research Institute, 26 Songdomirae-ro, Incheon 21990, Republic of Korea (changkun@kopri.re.kr), [2]Oil & Gas Research Center, Korea Institute of Geoscience and Mineral Resources, Daejeon 34132, Republic of Korea.

Introduction: Primitive chondrites preserve physico-chemical processes in the protoplanetary disk. However, they have experienced secondary processes such as aqueous alteration, thermal metamorphism, and shock metamorphism on their parent bodies, which could have modified primary chemical and isotopic signatures of the chondritic components. Thus, it is important to identify primitive chondrites that had experienced minimal parent body processes. The petrologic subtype (from 3.0 to 3.2) of unequilibrated ordinary chondrites (UOCs) can be determined by Cr_2O_3 content in ferroan olivine (FeO wt% > 2) [1], the maturation of the organic matter in the matrix [2], and number density Ni-rich metal in chondrule [3]. A small number of primitive ordinary chondrites have been identified so far. Here we report a primitive ordinary chondrite Elephant Moraine (EET) 14017, which is classified as LL3.05-3.10.

Methods: A polished thin section (PTS) of EET 14017 was studied for petrography, mineral chemistry, Raman spectroscopy. A field emission electron microprobe (JEOL JXA-8530F) at Korea Polar Research Institute was utilized with a 15 keV accelerating voltage, 10 nA beam current, and beam size of ~1 μm for BSE imaging, x-ray mapping, and quantitative analysis. The Raman experiments were performed at Thermo Fisher Scientific Korea with a DXR2xi equipped with an argon ion laser and using 532 nm excitation. The laser beam was focused on the samples by a 100× objective, leading to a ~1 μm diameter spot. The power of the laser was tuned as 0.5 mW (on the sample surface, measured out of a 10× objective). Acquisition consisted of ~0.1 s exposer time with 600 scans. Raman spectra were obtained from the PTS in the spectral region 800–2500 cm^{-1}, covering the first order carbon bands.

Results: Stereomicroscopic image and a combined false color x-ray map of the PTS show that chondrules of EET 14017 are clearly defined (Fig. 1). The optical and textural features of olivine, like sharp optical extinction and irregular fractures suggest S1 shock stage for EET 14017. The observed minor oxide veins and rims around metal and troilite in EET 14017 indicate the weathering classification of W1.

The content of chondrule in EET 14017 is ~80 vol%. The metal content is low (< 1 vol%) and the matrix content is ~15 vol%. Chondrules are diverse in sizes, mineral compositions, and textures including radial pyroxene, porphyritic olivine, poikilitic pyroxene-olivine, barred olivine, and cryptocrystalline chondrules. The size of chondrules varies from ~0.4 to ~2.6 mm with an average of 0.9 mm. Chondrules retain glassy mesostases and/or quenched textures. No Ca-Al-rich inclusions are found, although four Al-rich chondrules are identified in the PTS.

Fa content of olivine in EET 14017 is highly variable, ranging from ~1 to ~32 mol%, with an average of 14 mol% with a percent mean deviation (PMD) of 57%. The fs content of pyroxene in EET 14017 is 15 mol% in average with a PMD of 54%. The plagioclase is observed in ten chondrules. One of the plagioclase-rich chondrules in EET 14017 show co-occurrence of lath-shaped and interstitial plagioclase, which was investigated with Raman spectroscopy in the previous study [4]. Minor amount of spinel and chromite are also present in some chondrules. A pure spinel ($MgAl_2O_5$) is observed in one chondrule. Chromite appears as a small crystal in chondrules but also in the matrix, often in the form of anhedral clusters or as tiny isometric grains. Fe-Ni metal spherules in type I chondrules generally show Ni-rich metal within kamacite. Plessitic intergrowth in Fe-Ni metal spherules were not observed in EET 14017, which is typical in Semarkona [3]. Cristobalite is observed in one radial pyroxene chondrule (Fig. 2).

Discussion: The high abundance of chondrules (~80 %), variable but relatively large chondrule sizes, and metal abundance (less than 1 vol%) indicate that EET 14017 is a LL chondrite. The Fa contents of olivine in EET 14017 is consistent with those for petrologic type 3 UOCs, and the 57% percent mean deviation (PMD) (Dodd et al., 1967) of the FeO content indicates a petrologic type < 3.1 [5]. The average of Cr_2O_3 contents from ferroan olivines in EET 14017 is 0.43 ± 0.18 wt% (Fig. 3). The standard deviation and the mean of the Cr_2O_3 content of the ferroan olivines in EET 14017 are comparable to those from type 3.05-3.10 UOCs [1]. The FWHM of the D band of Raman spectra for polyaromatic carbonaceous matter in matrix of EET 14017 is plotted against the ratio of the peak intensities for the D and G bands (I_D/I_G) (Fig. 4). The Raman spectral parameters of EET 14017 is comparable with those of Bishunpur (type 3.1) [2].

The cristobalite, high-temperature silica polymorph, in radial pyroxene chondrule suggests that the chondrule precursor formed by fractional condensation in the solar nebula and reheated to ~1100

- 2000 K during the chondrule formation [6]. The co-occurrence of lath-shaped plagioclase and interstitial plagioclase may indicate the complex cooling history the plagioclase-rich chondrules in EET 14017. Dynamic crystallization experiments from olivine-rich chondrule melts showed that lath-shaped plagioclase crystallized at faster cooling rates (>~50 °C/h) and interstitial plagioclase formed at slower cooling rates (<~10 °C/h) [7].

Conclusion: Based on the Cr_2O_3 content in ferroan olivines and Raman spectral data obtained from marix, EET 14017 is a primitive LL chondrite, petrological subtype of 3.05-3.10. Further mineralogical and isotopic studies for individual chondritic components in EET 14017 are required.

Acknowledgments: This study was supported by KOPRI grant PE23050.

References: [1] Grossman J. N. & Brearley A. J. (2005) *MaPS* 40, 87-122. [2] Bonal L. et al. (2016) *GCA* 189, 312-337. [3] Kimura M. et al. (2008) *MaPS* 43, 1161-1177. [4] Park S. Y. & Park C. (2019) *Spectrochim. Acta Part A* 207, 46-53. [5] Huss G. R. et al. (2006) *Meteorites and the Early Solar System II*, pp. 567-586. [6] Hezel D. C. et al. (2006) *GCA* 70, 1548-1564. [7] Tronche E. J. et al. (2007) *GCA* 71, 3361-3381.

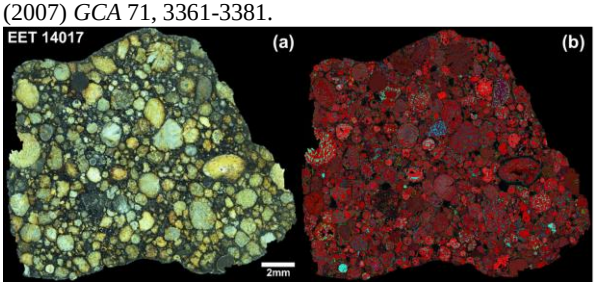

Figure 1. (a) Stereomicroscopic image and (b) combined false color map in Mg (red), Ca (green), Al (blue) Kα x-rays of EET 14017. The bright red, dark red, and sky blue color denotes olivine, pyroxene, and plagioclase, respectively.

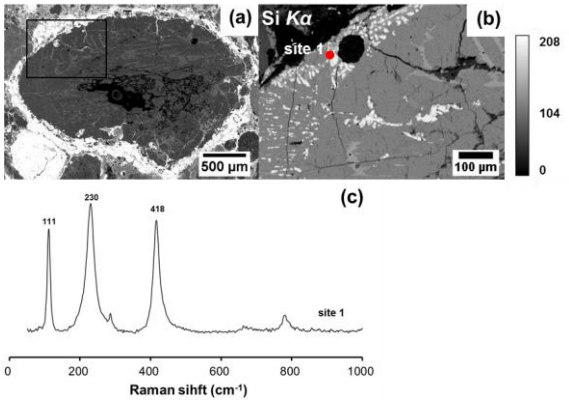

Figure 2. (a) Backscattered electron (BSE) image of silica bearing chondrule in EET 14017. (b) Si x-ray map of the black rectangle in (a). (c) Raman spectrum of cristobalite obtained from site 1 in (b).

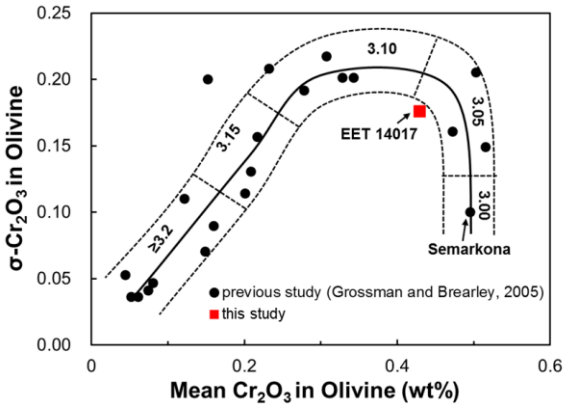

Figure 3. Histogram of the Cr_2O_3 content in ferroan chondrule olivine grains from EET 14017. The average value is 0.43 ± 0.18.

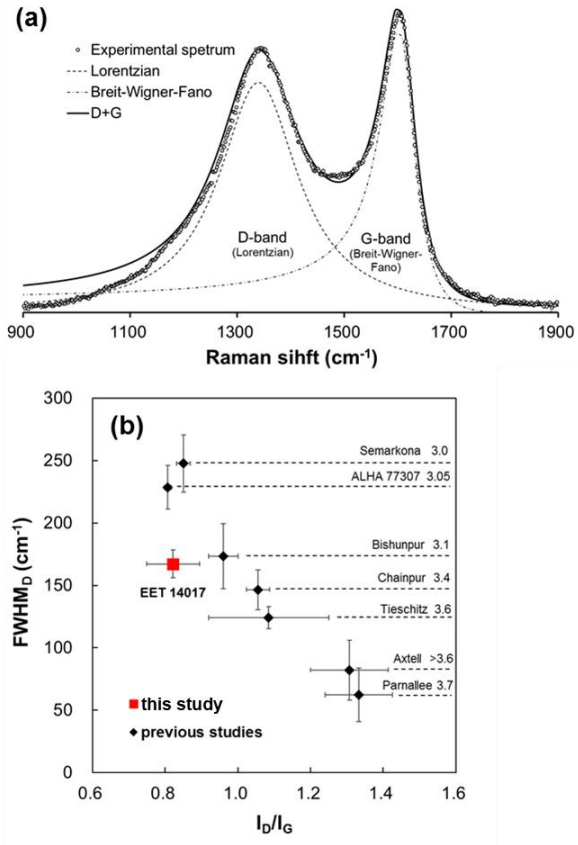

Figure 4. (a) Representative Raman spectra (900–1900 cm^{-1}) of polyaromatic carbonaceous matter present in the matrix of EET 14017 using 532 nm laser. The actual Raman probe spot size was 1.4 µm). The G and D-bands were fitted with a Breit-Wigner-Fano (BWF) and a Lorentzian profiles, respectively. (b) A plot of the full-width at half-maximum (FWHM) of the Raman D band (cm^{-1}) versus the ratio of peak intensities for the D and G bands, I_D/I_G.